File

CHAPTER

8

ULTRASENSITIVE MICROARRAY DETECTION OF DNA USING ENZYMATICALLY AMPLIFIED SPR IMAGING

HYE JIN LEE, ALASTAIR W. WARK, AND ROBERT M. CORN

PROOF

8.1. INTRODUCTION

The use of surface bioaffinity interactions in a microarray format has become an indispensable tool for modern biological research. Measurements of DNA–DNA hybridization, protein–DNA binding, and antibody–antigen interactions can all be performed now with biopolymer microarrays that permit the simultaneous characterization of multiple bioaffinity binding processes. In particular, DNA microarrays currently provide researchers with a simple and systematic method for the simultaneous identification and quantification of multiple nucleic acid sequences in a sample for a variety of applications, including gene expression analysis (Lockhart and Winzeler, 2000; Stears et al., 2003; Nelson et al., 2004; Thomson et al., 2004), single nucleotide polymorphism (SNP) profiling (Gerry et al., 1999; Kwok, 2001; Gerion et al., 2003; Giusto and King, 2003; Zhong et al., 2003), and the detection of specific viral and bacterial species (Wang et al., 2002; Sengupta et al., 2003; Volokhov et al., 2003; Gonzalez et al., 2004; Lin et al., 2004; Chen et al., 2005). The selectivity and reliability of DNA microarrays are usually determined by the sequence specificity of the surface hybridization of target DNA or RNA from solution onto the various DNA or RNA microarray elements.

Fluorescence microscopy is the most commonly used approach for biosensing with DNA microarrays (van Hal et al., 2000; Zammatteo et al., 2000; Epstein et al., 2002; Lehr et al., 2003; Livache et al., 2003; Stears et al., 2003; Stoughton, 2005). If a fluorescent tag is attached to one end of a single-stranded DNA (ssDNA) molecule, the hybridization of this target ssDNA onto a microarray element that contains specific complementary probe oligonucleotides can be detected with a fluorescent imaging experiment. For example, this type of measurement is the basis for the analysis of the large-scale photolithographically generated microarrays employed by Affymetrix ()(Pease et al., 1994; Schena et al., 1995; Winzeler et al., 1998; Brenner et al., 2000; Berchuck et al., 2005).

For cases where labeling is not possible or not desired, the surface-sensitive optical technique of surface plasmon resonance imaging (SPRI) is an excellent alternative for the detection of surface bioaffinity measurements with biopolymer microarrays (Lyon et al., 1999; Brockman et al., 2000; Smith and Corn, 2003; Wegner et al., 2004a; Lee et al., 2005d). SPRI measures biopolymer adsorption onto a surface by detecting any changes in the local index of refraction that occur upon binding events. SPR imaging has been applied to the

New Frontiers in Ultrasensitive Bioanalysis. Edited by Xioa-Hong Nancy Xu
Copyright © 2007 John Wiley & Sons, Inc.

detection of DNA–DNA (Lee et al., 2001; Nelson et al., 2001; Smith et al., 2002). RNA–DNA (Nelson et al., 2002; Goodrich et al., 2004a,b), DNA–protein (Smith et al., 2003a; Kyo et al., 2004; Shumaker-Parry and Campbell, 2004; Shumaker-Parry et al., 2004; Okumura et al., 2005), peptide–protein (Wegner et al., 2002; Wegner et al., 2004b), carbohydrate–protein (Smith et al., 2003b), and antibody–antigen (Wegner et al., 2003; Kanda et al., 2004; Wilkop et al., 2004) binding in a microarray format. SPRI is also potentially a superb candidate for the direct analysis of genomic DNA and RNA in an array format without labeling or PCR amplification. However, to date the application of SPRI to genomic DNA samples has not been possible due to a concentration limit of 1 nM for the detection of short (16–20mer) oligonucleotides; genomic DNA samples typically have DNA concentrations of approximately 20 fM (Goodrich et al., 2004a).

In fact, a target DNA concentration of 20 fM is also too small to be detected directly in a typical fluorescent imaging experiment. An amplification method must be used to increase the sensitivity of the surface bioaffinity measurement; typically a small amount of a particular DNA fragment in a genomic sample is enzymatically amplified using the polymerase chain reaction (PCR) with a fluorescent tag attached to one of the PCR primers (Sengupta et al., 2003; Gonzalez et al., 2004). For large sets of DNA molecules, simultaneous PCR amplification is not possible. For these systems, sandwich assays involving three oligonucleotides and either enzymes or nanoparticles have been proposed as a means of amplifying the signal (Kawai et al., 1993; Morata et al., 2003; Storhoff et al., 2004; Bao et al., 2005). Some of these amplification methods have also been used in conjunction with SPRI (He et al., 2000).

Recently, we have developed a novel surface-based enzymatic process that can be used to lower the limit of detection for SPRI measurements of ssDNA to a concentration of 1 fM. This enzymatically amplified SPR imaging method can be used for the direct detection of specific sequences from human genomic DNA. In this method, RNase H is used in conjunction with RNA microarrays for the enzymatically amplified detection of DNA. In this chapter we describe in detail this method for the ultrasensitive detection of DNA with enzymatically amplified SPRI.

This chapter is divided into four sections. In Section 8.2, we describe the SPRI measurement in detail and discuss how to make DNA and RNA microarrays on chemically modified gold surfaces. In Section 8.3, we examine the use of SPRI for the direct detection of DNA, and what limits the sensitivity of this method to 1 nM. In Section 8.4, we introduce the surface RNase H hydrolysis reaction that serves as the core of the enzymatic amplification process, and we show what experiments and analyses are required to completely characterize surface enzyme reactions. Finally, in Section 8.5, we show how enzymatically amplified SPRI can be used to detect femtomolar concentrations of oligonucleotides, PCR products, and unamplified genomic DNA directly.

8.2. OVERVIEW OF SPRI METHODOLOGY

Surface plasmon resonance (SPR) is a surface-sensitive optical technique that can be applied to the real-time monitoring of biomolecular adsorption and/or desorption events at biopolymer layers formed on a thin gold film or other noble metal surfaces. Surface plasmons are electromagnetic waves that propagate along a metal/dielectric interface. The optical field intensity of the surface plasmon waves decays exponentially from the surface of the metal into the dielectric layer. For a gold film, this decay length is about 200 nm, thus defining a region where the SPR response is sensitive to localized changes in refractive index due to

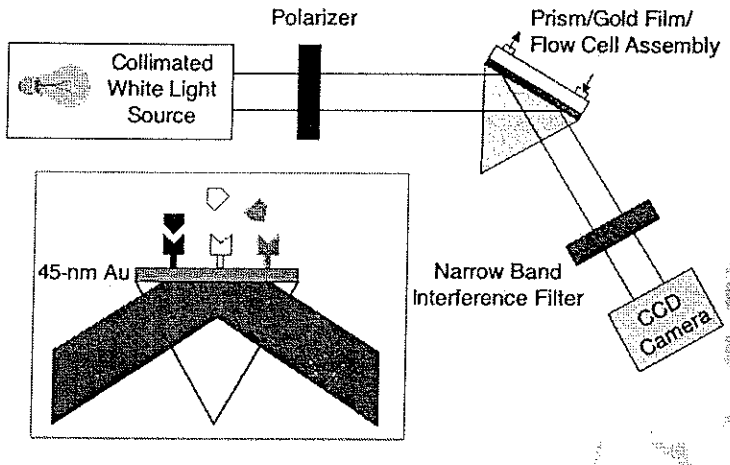

Figure 8.1. Schematic overview of the SPRI apparatus. Inset is a representation of the analyte/thin gold film/prism assembly.

the adsorption or desorption of molecules. Surface plasmons cannot be excited directly by light at planar air–metal or water–metal interfaces because momentum-matching conditions are not satisfied. Instead, a diffraction grating or prism arrangement, such as that shown in Figure 8.1, is required to convert incident p-polarized light photons into surface plasmons (Hanken et al., 1998; Knoll, 1998; Homola et al., 1999). Changes in the SPR response can be measured using three different instrumental formats: (1) scanning angle SPR, (2) scanning wavelength SPR, and (3) SPR imaging. Angle shift measurements (Szabo et al., 1995; Chinowsky et al., 2003) are the most commonly undertaken technique and form the basis of the commercial instruments available from Biacore and Texas Instruments. In scanning angle SPR, the reflectivity of monochromatic incident light is monitored as a function of incident angle, while in scanning wavelength SPR (Frutos et al., 1999; Corn and Weibel, 2001), it is the incident angle that remains fixed. The latter approach is the principle behind the Fourier Transform SPR instrument available from GWC Technologies. Both of these techniques are used to study a single region on a gold surface. In contrast, SPR imaging measurements simultaneously monitor spatially resolved changes in reflectivity at a fixed angle and wavelength due to biomolecular adsorption onto an array surface. Commercial SPR imaging instruments are available from GWC Technologies and HTS Biosystems.

The high-throughput capabilities of SPRI make it an attractive tool for studies involving the screening of multiple biomolecular interactions on a single chip surface. Figure 8.1 shows a schematic representation of the SPR imaging instrument used to detect the adsorption of biopolymers in solution zo surface-immobilized biomolecules such as DNA (Nelson et al., 2001; Kyo et al., 2004), RNA (Goodrich et al., 2004a,b), peptides (Wegner et al., 2002, 2004b), carbohydrates (Smith et al., 2003b), and proteins (Wegner et al., 2003; Kanda et al., 2004).

The output from a collimated white light source is first passed through a polarizer before being directed through a high-index prism/sample assembly at an optimal incident angle. The p-polarized light impinges on the back of a gold thin film, whose surface is chemically modified with an array of biomolecules. The reflected light is then collected via a narrow band-pass filter centered at 830 nm onto a CCD camera. Molecules are delivered to the gold surface using a flow cell with adsorption at a particular array element, resulting in an increase in reflectivity. This is detected by subtracting images acquired before and after the

surface binding event. For measured changes in percentage reflectivity ($\Delta\%R$) under 10%, a linear relationship exists between $\Delta\%R$ and the corresponding change in refractive index (Nelson et al., 2001). This relationship can also be applied to determine the surface coverage of biomolecules adsorbed onto the surface, thus allowing the use of SPRI to quantitatively evaluate the binding affinity between the biomolecules in solution and the multiple probes immobilized on the array.

8.2.1. Surface Attachment Chemistry

The use of well-characterized and robust surface chemistries to tether biological molecules onto gold surfaces in an array format is an essential component of a successful SPRI experiment. Because noble metal films are required for the propagation of surface plasmons, commercially available DNA arrays created on glass substrates, such as those provided by Affymetrix or inkjet printing processes (Winzeler et al., 1998; Hughes et al., 2001; Berchuck et al., 2005), cannot be utilized. Consequently, we have developed a strategy using self-assembled alkanethiol monolayers (SAMs) containing an ω-terminated amine functional group as the foundation of the array. Thiol-modified biomolecules such as thiol-modified DNA (Brockman et al., 1999), RNA (Goodrich et al., 2004a,b), carbohydrates (Smith et al., 2003b), and cysteine-containing peptides (Wegner et al., 2002) can then be covalently attached to the surface through the use of heterobifunctional linker molecules such as SSMCC (sulfosuccinimidyl 4-(*N*-maleimidomethyl) cyclohexane-1-carboxylate) and SPDP (*N*-succinimidyl 3-(2-pyridyldithio)-propionamido). This approach has been successfully applied to create equally robust DNA, RNA, and peptide microarrays.

Figure 8.2 shows two different reaction schemes for the surface immobilization of thiol-modified probe molecules. In the first approach, the *N*-hydroxysulfosuccinimide (NHS)

Au: Labels (a) and (b) ok where added in art?

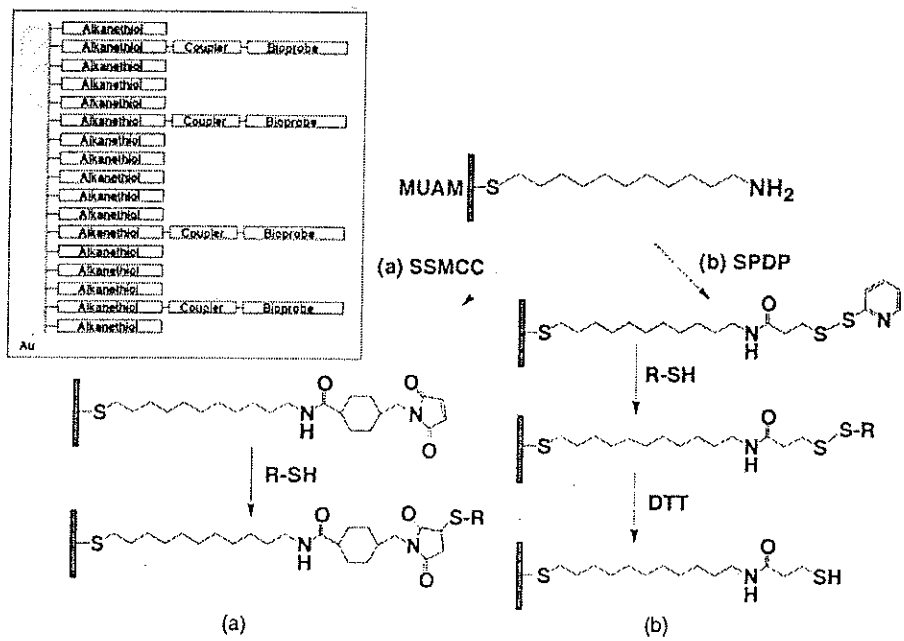

Figure 8.2. Reaction schemes outlining two different surface attachment chemistries [(a) SSMCC and (b) SPDP] for the surface immobilization of thiol-modified probe biomolecules.

ester moiety of SSMCC is reacted with a densely packed SAM of 11-mercapto-undecylamine (MUAM) to form an amide bond, leaving the free maleimide group to react with a thiol-modified biomolecule (Figure 8.2a). Alternatively, a MUAM monolayer is reacted with the molecule SPDP, resulting in the creation of a surface terminated with pyridyl disulfide groups (Figure 8.2b). Thiol-modified oligonucleotides (both DNA and RNA) are then attached via a thiol-disulfide exchange reaction with pyridine-2-thione as the leaving group. The SPDP chemistry has the advantage of being reversible as compared to SSMCC; the disulfide bond can be cleaved in the presence of dithiothreitol to regenerate the sulfhydryl-terminated surface. The thiol-modified probe oligonucleotides used are typically single-stranded and consist of 16–20 bases with a spacer between the C6-thiol modifier and the probe sequence. This spacer is designed to improve the accessibility of the surface attached molecule to the target molecule in solution. Examples of spacers employed include 15 thymine bases, $(T)_{15}$, or 12 ethylene glycol molecules, $(EG)_{12}$, for DNA and eight uracil bases, $(U)_8$, for RNA probes. In addition, surfaces fabricated using these approaches are very stable and can be used for several assay cycles as well as for allowing good control over the surface density of probe molecules. For example, the hybridization of target DNA onto ssDNA microarrays (16mer short oligonucleotides) followed by regeneration of the array by washing with 8 M urea can be repeated up to 20 times (Lee et al., 2001; Nelson et al., 2001; Wark et al., 2005). Both attachment chemistries (SSMCC and SPDP) provide a typical ssDNA monolayer surface coverage of approximately 5×10^{12} molecules/cm^2.

8.2.2. Array Fabrication

The fabrication of arrays containing multiple, independently addressable elements on a single gold surface for use in SPRI measurements can be achieved using a combination of self-assembly, surface attachment chemistry, and array patterning. Two different array fabrication methods have been developed in our laboratory: (i) UV photopatterning in combination with a series of chemical modification steps allowing the production of relatively large numbers (> 100) of array elements (Brockman et al., 1999) and (ii) the use of polydimethylsiloxane (PDMS) microfluidic networks which are physically sealed onto the chemically modified gold surface (Lee et al., 2001).

Spotted Microarrays. (Brockman et al., 1999). The first step of the fabrication method is the reaction of the MUAM modified gold surface with the *N*-hydroxysuccinimide ester of 9-fluorenylmethoxycarbonyl (Fmoc-NHS), which serves as a hydrophobic protecting group. By exposing the Fmoc surface to UV radiation through a quartz mask containing 500-μm^2 features, patterns of bare gold spots surrounded by the hydrophobic background were created. The slide is then immersed again in an ethanolic MUAM solution for 2 hours, with the resulting MUAM patches then reacted with a heterobifunctional linker, SSMCC or SPDP, followed by thiol-modified oligonucleotides. Each of the array elements is separately addressed using a manually operated picopump to spot SSMCC or SPDP and thiol-modified probes (DNA or RNA) onto the surface. This approach is successful because the hydrophobic Fmoc background ensures that each droplet is contained on a particular array element, thus avoiding cross contamination of other sequences on neighboring elements. The Fmoc background can be completely removed with a mildly basic solution and the regenerated MUAM surface reacted with an NHS derivative of polyethylene glycol (PEG-NHS) to create a background resistant to nonspecific adsorption of biomolecules. Figure 8.3a shows an example of a raw SPR image of an array fabricated using this procedure with over 110

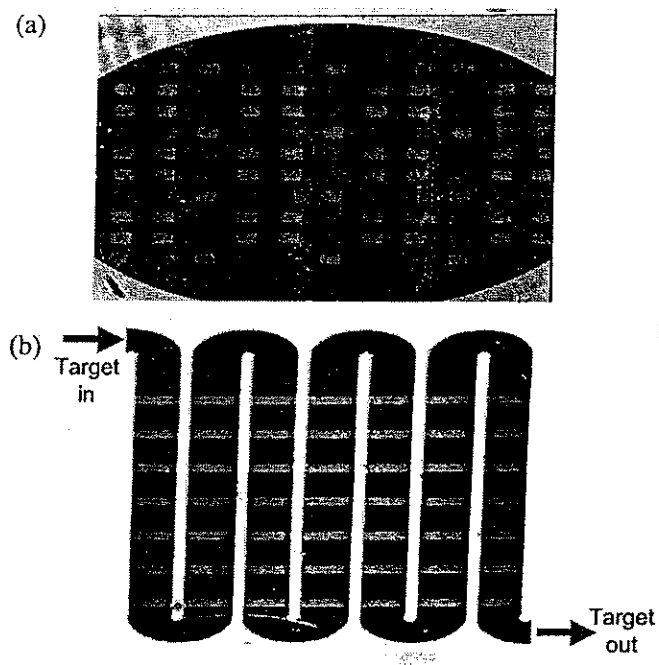

Figure 8.3. SPR raw images showing (a) an array fabricated using a multistep chemical protection/deprotection process in conjunction with UV photopatterning using a mask featuring a 500-μm square pattern. (b) The line array was created using a set of parallel PDMS microfluidic channels to deliver linker and probe molecules before being replaced by a second serpentine PDMS channel to create a continuous-flow cell.

individual elements. Furthermore, if a 250-μm^2 photomask is used instead, it is possible to attain over 300 elements on a single microarray surface.

Microfluidic Line Arrays. (Lee et al., 2001). A second approach involves the coupling of PDMS microfluidic channels to the gold surface for use in SPRI measurements with the aim of reducing chemical consumption and sample volume as well as speeding up analysis times. First, a set of parallel microchannels (300-μm width, 14.2-mm length, 35-μm depth) with 700-μm spacing between channels is created by replication from a 3-D silicon wafer master using soft lithography methods (Lee et al., 2001). The PDMS microchannels are then physically attached onto a MUAM modified gold surface before the heterobifunctional cross-linker (SSMCC or SPDP) and thiol-modified DNA or RNA are sequentially passed through using a simple differential pumping system to create a series of individual line elements on the gold array surface. After the surface immobilization of probe molecules is complete, the channels are removed and the background MUAM monolayer that surrounds the channels is reacted with PEG-NHS, with no other chemical protection and deprotection steps required. By changing the spacing and widths of the microchannels, a single chip can contain a maximum of 100 different probe elements.

In order to achieve a continuous flow of sample to the surface array for kinetics measurements, the large flow cell (100 μl) used in Figure 8.3a is replaced with a second PDMS microchannel (see Figure 8.3b). The serpentine design (670-μm width, 9.5-cm length, 200-μm depth, ~10-μL total volume) facilitates well-controlled and reproducible sample

delivery to each array element as well as significantly reducing the sample volume. Discrete SPR imaging probing regions are formed by orienting the microchannel perpendicular to the probe line array. The microchannel is created by replication from a 3-D aluminum master (Wegner et al., 2004b). SPR imaging kinetics experiments are performed using a continuous flow of solution through the serpentine microchannel to prevent mass transport limitations, while equilibrium measurements are obtained under stopped-flow conditions using the large flow cell. Additionally, a constant temperature sample holder encased in a specially designed water jacketed cell, allowing the system temperature to be controlled to within 0.1°C, is used to reduce fluctuations in SPR signal due to temperature variations (Goodrich et al., 2004b; Lee et al., 2005a). Finally, if the simultaneous injection of multiple samples is desired, a set of parallel PDMS microchannels placed perpendicular to the line array can be used to deliver 1–2 μL of target sample per channel (Lee et al., 2001).

8.3. DIRECT DETECTION OF DNA BY HYBRIDIZATION ADSORPTION

The direct analysis of genomic DNA and RNA in an array format without labeling or PCR amplification would be extremely advantageous for a variety of biological applications. The detection and identification of ssDNA oligonucleotides by sequence specific adsorption onto an ssDNA microarray element to form a double-stranded duplex is called hybridization adsorption. If the target oligonucleotide is labeled with a fluorophore, fluorescence imaging can be used to detect DNA with the microarray. If the DNA has no fluorescent tag, then SPRI can be used to directly detect DNA hybridization adsorption. SPR imaging measurements of DNA microarrays has been demonstrated previously by a number of research groups (Guedon et al., 2000; Nelson et al., 2001; Livache et al., 2003; Rella et al., 2004; Shumaker-Parry et al., 2004; Okumura et al., 2005; Wark et al., 2005). However, the detection limit for DNA or RNA analysis via hybridization adsorption of untagged target molecules typically lies in the nanomolar range (Guedon et al., 2000; Nelson et al., 2001; Livache et al., 2003; Okumura et al., 2005; Wark et al., 2005). A typical sample of genomic DNA (35 μg/mL) has a ssDNA concentration of around 20 fM. What can be done to improve the SPRI methodology to increase its sensitivity into the femtomolar range?

To answer this question, we must carefully examine the thermodynamic and kinetic limitations of surface bioaffinity measurements. An example of the detection of DNA by hybridization adsorption onto DNA microarrays with SPRI is shown in Figure 8.4. A four-component ssDNA microarray is exposed to two of the complementary DNA target sequences, with only the perfectly matched array elements forming duplexes via hybridization adsorption (Figure 8.4b). A positive increase in percent reflectivity ($\Delta\%R$) due to selective hybridization adsorption is observed; Fresnel calculations and experimental evidence show that if the SPRI response remains below 10%, then it is directly proportional to the relative surface coverage (θ) of complementary DNA (Nelson et al., 2001), where $\theta = \Gamma/\Gamma_{\text{tot}}$ and Γ represents the molecular surface density. θ is related to the bulk concentration (C) of ssDNA by the Langmuir adsorption isotherm:

$$\theta = K_{\text{Ads}}C/(1 + K_{\text{Ads}}C), \tag{8.1}$$

where K_{Ads} is the Langmuir adsorption coefficient. A typical Langmuir isotherm for 16mer adsorption is shown in Figure 8.4c. At a bulk concentration of $C_{0.5} = 1/K_{\text{Ads}}$, the relative surface coverage is 0.5. For a 16mer DNA, $K_{\text{Ads}} = 2 \times 10^7\ \text{M}^{-1}$, so that $C_{0.5}$ is at 50 nM.

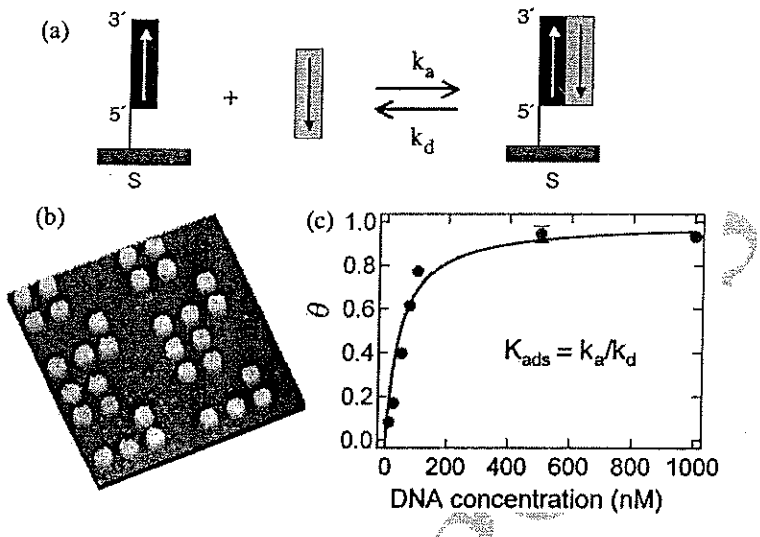

Figure 8.4. (a) Schematic representing DNA hybridization adsorption onto DNA or RNA microarrays. (b) An example of an SPR difference image showing the sequence-specific hybridization/adsorption of target DNA onto a four-component ssDNA microarray. This was obtained by exposing the ssDNA array to a 500 nM solution containing two different target DNA sequences with duplex formation occurring only at the complementary probe array elements. A maximum of 130 individually addressable array elements on a single chip with a total surface area of 0.8 cm^2 can be created using a 500-μm^2 photopatterning mask. (c) An example showing a plot of the relative surface coverage (θ) as a function of target complementary DNA concentration. The solid line represents a Langmuir isotherm fit to the data. A value of $K_{ads} = 2.0\ (\pm\ 0.2) \times 10^7\ M^{-1}$ was determined from the fit.

Comparable K_{Ads} values have been observed with both fluorescence imaging and SPR measurements (Liebermann et al., 2000; Nelson et al., 2001; Peterson et al., 2002; Lee et al., 2005a; Levicky and Horgan, 2005; Wark et al., 2005).

At low surface coverages, the Langmuir isotherm depends linearly on the target DNA concentration:

$$\theta = K_{Ads} C. \tag{8.2}$$

Equation (8.2) shows one reason why it is difficult to measure 1 fM target concentrations with a surface bioaffinity measurement: As C goes to zero, θ goes to zero as well! If one wants to detect ssDNA at a bulk concentration of 1 fM, then one must be able to detect a relative surface coverage of $\theta = 2 \times 10^{-8}$! As mentioned in the previous section, the surface density of DNA probes on a microarray element is typically 5×10^{12} molecules/cm^2, so that the surface density of dsDNA is $\Gamma = 10^5$ molecules/cm^2 at 1 fM. For a 500-μm array element, this corresponds to 250 molecules; for a 50-μm array element, this surface density corresponds to 2.5 molecules!! SPRI typically has a detection limit of 1 nM for 16mer oligonucleotide adsorption, which corresponds to a lowest relative surface coverage of $\theta \sim 2 \times 10^{-2}$ or $\Gamma \sim 10^{11}$ molecules/cm^2. If a sandwich assay is used with a DNA-coated nanoparticle, a relative surface coverage of $\theta \sim 2 \times 10^{-4}$ corresponding to a detection limit of approximately 10 pM is observed (He et al., 2000). For comparison, a typical lowest surface coverage that can be observed above background for the detection of DNA in a sandwich assay with a fluorescently tagged DNA molecule is $\Gamma \sim 10^8$ molecules/cm^2, corresponding to a detection limit of approximately 1 pM (Zammatteo et al., 2000; Lehr et al., 2003; Livache et al., 2003).

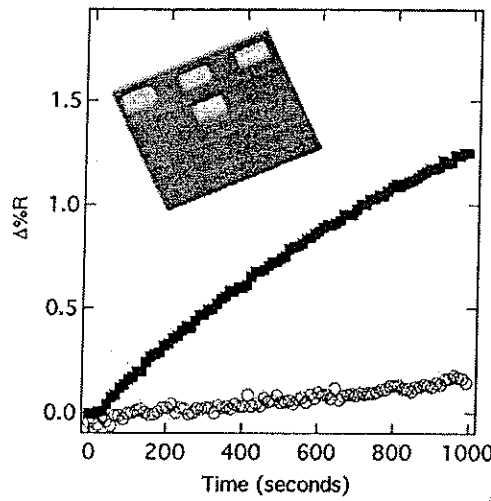

Figure 8.5. Representative real-time SPRI curves showing sequence specific hybridization adsorption of complementary DNA onto a surface probe element at concentrations of 1 nM (O) and 10 nM (■). The figure inset is an SPR difference image obtained by subtracting images acquired before and after the hybridization adsorption of 100 nM target DNA onto DNA array elements corresponding to a final $\Delta\%R$ change of 2%. [Reprinted with permission from *Anal. Chem.* 77:5096–5100, Copyright 2005, American Chemical Society.]

A second reason that it is difficult to detect a 1 femtomolar solution of ssDNA with SPRI hybridization adsorption measurements is the kinetics of hybridization adsorption. The hybridization adsorption rate (k_a) for a 16mer was measured to be approximately $10^5 M^{-1}s^{-1}$ from the data in Figure 8.5. Since the velocity of the adsorption reaction is $k_a C$, this rate decreases significantly as the concentration is lowered. Moreover, there is also a diffusional contribution that becomes significant at lower concentrations due to the time required for the molecules to reach the surface. These two effects are observed in Figure 8.5, which shows the time-dependent SPRI responses upon exposure of an ssDNA array to 10 and 1 nM solutions of complementary 16mer DNA. The initial adsorption rate, as determined from the initial slopes, decreases by a factor of 10 as the target DNA concentration is decreased from 10 to 1 nM, as expected from simple Langmuir kinetics. Thus, due to both Langmuir adsorption equilibrium arguments and adsorption kinetics, the detection limit for the direct detection of ssDNA oligonucleotides with SPRI is estimated to be 1 nM. To analyze genomic DNA at a concentration of 1 fM with SPRI, an amplification methodology is required. While an ELISA-based amplification scheme may provide sufficient sensitivity (Kawai et al., 1993; Morata et al., 2003), we will choose a different strategy for DNA detection, employing RNase H in conjunction with RNA microarrays to create a new type of surface enzyme amplification scheme.

8.4. RNASE H SURFACE ENZYME KINETICS

RNase H is an endoribonuclease that selectively hydrolyzes the RNA strand of an RNA–DNA heteroduplex (Nakamura et al., 1991; Katayanagi et al., 1993; Zamaratski et al., 2001). Figure 8.6 shows a schematic drawing of the two possible ways that RNase H can react with surface-bound RNA–DNA heteroduplexes. The heteroduplex is first formed on

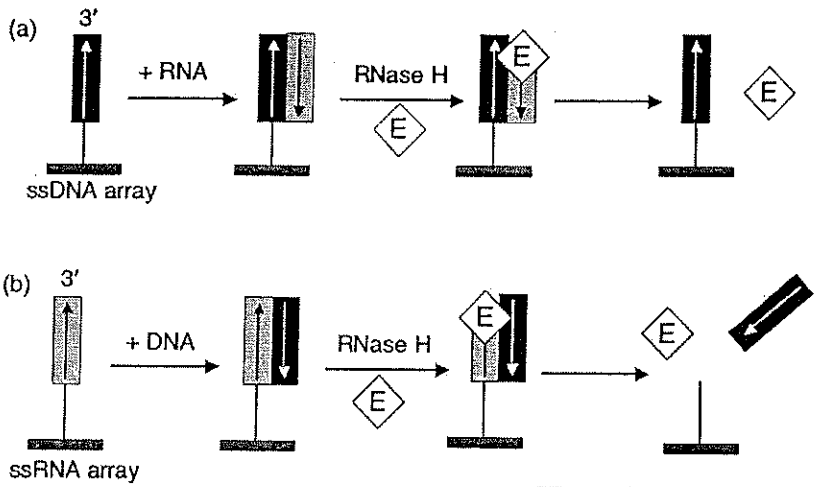

Figure 8.6. Schematic representation of RNase H activity at surface-bound RNA–DNA heteroduplexes formed by hybridization adsorption of (a) target RNA onto ssDNA microarrays and (b) target DNA onto ssRNA microarrays.

the surface of either a DNA or RNA microarray (see Figures 8.6a and 8.6b, respectively) by hybridization adsorption of the complementary oligonucleotide from solution. After hybridization, the RNA strand of the heteroduplex will be hydrolyzed and destroyed by RNase H. In the case of the DNA microarray (Figure 8.6a), hydrolysis leaves the original ssDNA still attached to the surface and capable of hybridization adsorption. In contrast, the RNase H hydrolysis of the RNA microarray results in both the destruction of the surface array element and the release of the target DNA back into solution (Figure 8.6b).

To demonstrate this surface RNase H activity, a series of real-time SPR imaging measurements were obtained for the reaction of RNase H with RNA–DNA heteroduplexes formed on DNA and RNA microarrays. Figure 8.7 plots the real-time SPRI signal for both cases (labeled a and b, respectively). A rapid rise in $\Delta\%R$ to a steady-state value of $+1.6\%$ was observed upon the hybridization adsorption of DNA or RNA onto the surfaces from 500 nM complement solutions. Subsequent rinsing of the DNA and RNA microarrays with buffer followed by exposure to RNase H resulted in a rapid decrease in $\Delta\%R$ from the hydrolysis of the RNA on the surface. For the case of the DNA microarray, a $\Delta\%R$ of -1.6% was observed; this decrease brought the SPRI signal back to the original reflectivity level prior to hybridization adsorption and suggests that the RNase H completely removed all surface-bound RNA. In contrast, for the case of the heteroduplexes formed using RNA microarrays, a decrease of -3.2% was observed corresponding to the complete loss of both the target DNA and probe RNA from the surface. No hybridization adsorption was observed upon subsequent exposure of the RNA microarray to complementary ssDNA. Moreover, if the experiments were repeated after the creation of either surface-bound dsDNA or dsRNA, no surface enzymatic hydrolysis was observed. These additional measurements confirmed the selectivity and specificity of the surface RNase H reaction to the RNA–DNA heteroduplex.

How does one quantify the reaction rate of the RNase H surface hydrolysis process? The characterization of the surface enzyme reactions utilized in biosensing processes is extremely important for optimization of the array-based biosensor, because an enzyme reaction can be orders of magnitude slower on a surface as compared to solution due to

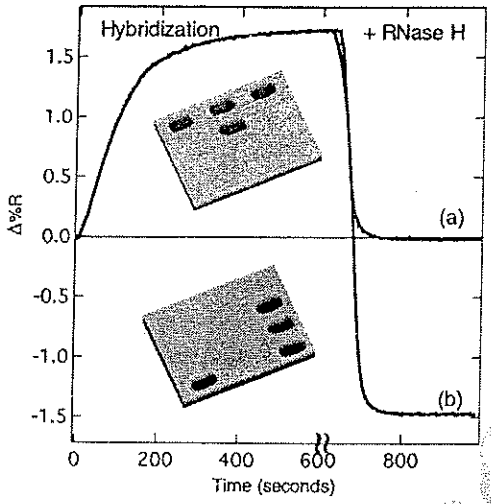

Figure 8.7. Real-time SPRI curves representing the sequence specific hybridization adsorption of (a) a 500 nM solution complementary RNA onto an ssDNA microarray and (b) a 500 nM solution of complementary DNA onto an ssRNA microarray. The surface hydrolysis of both DNA–RNA heteroduplexes (a) and (b) was monitored at an RNase H concentration of 8 nM. The figure insets are representative SPR difference images obtained by subtracting images acquired before and after RNase H hydrolysis of heteroduplexes formed in parts a and b.

a variety of transport and energetic factors. We have recently shown (Fang et al., 2005; Lee et al., 2005b) that a simple model can be used to describe surface enzyme reaction dynamics, such as the surface RNase H hydrolysis process that forms the foundation of our enzymatically amplified SPRI measurements.

A general reaction scheme for the enzymatic processing of a biopolymer microarray that couples diffusion, adsorption, desorption and surface catalysis is shown in Figure 8.8.

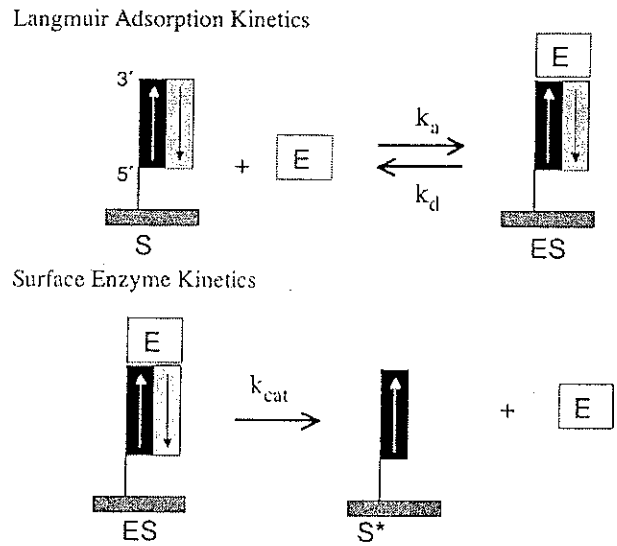

Figure 8.8. A reaction scheme outlining the surface enzymatic processing of a biopolymer microarray.

The enzyme (E) first adsorbs from solution onto the surface-bound substrate (S) to create a 1:1 surface complex (ES). The surface complex then reacts to form the surface-bound product (S^*) and releases the enzyme back into solution. This reaction scheme differs from the typical ELISA-based enzymatic method for detecting species on surfaces, which uses a sandwich assay in which an enzyme–protein conjugate binds to an adsorbed molecule and then reacts with a substrate in solution to create an amplified detection signal (Crowther, 1995). For the case of surface enzyme kinetics, the substrate is attached to the surface, and upon reaction of the surface complex, the enzyme is released back into solution.

The model shown in Figure 8.8 can be quantified with three rate constants (k_a, k_d, and k_{cat}) and an additional parameter (β) which describes the steady-state diffusion of enzyme to the surface. We rewrite the model for the surface enzyme reaction here in Equations (8.3)–(8.5):

$$E_{(x=\infty)} \xrightarrow{k_m} E_{(x=0)} \tag{8.3}$$

$$S + E_{(x=0)} \underset{k_d}{\overset{k_a}{\rightleftarrows}} ES \tag{8.4}$$

$$ES \xrightarrow{k_{cat}} S^* + E_{(x=0)} \tag{8.5}$$

where $E_{(x=\infty)}$ and $E_{(x=0)}$ are the bulk and surface enzyme species respectively, k_m is the steady-state mass transport coefficient, S is the RNA–DNA surface-bound substrate (the RNA–DNA heteroduplex), ES is the surface enzyme–substrate complex (the RNase H–heteroduplex complex), k_a and k_d are the Langmuir adsorption and desorption rate constants, S^* is the surface product (ssDNA), and k_{cat} is the surface reaction rate for the enzyme complex (Fang et al., 2005). The ratio k_a/k_d is the Langmuir adsorption coefficient K_{Ads}. The steady-state mass transport coefficient (k_m) can also be written as D/δ, where D is the diffusion coefficient for the enzyme and δ is the steady-state diffusion layer thickness (Bourdillon et al., 1999).

If the surface coverages for the three surface species S, ES, and S^* are denoted as Γ_S, Γ_{ES}, and Γ_{S*}, respectively, and the total number of surface sites is Γ_{tot}, then the surface kinetics equations can be expressed in terms of the relative surface coverages $\theta_x = \Gamma_x/\Gamma_{tot}$, where $x = S$, ES, or S^*:

$$\theta_S + \theta_{ES} + \theta_{S*} = 1 \tag{8.6}$$

$$\frac{d\theta_{ES}}{dt} = \frac{k_a[E]^b(1 - \theta_{ES} - \theta_{S*}) - (k_d + k_{cat})\theta_{ES}}{1 + \beta(1 - \theta_{ES} - \theta_{S*})} \tag{8.7}$$

$$\frac{d\theta_{S*}}{dt} = k_{cat}\theta_{ES} \tag{8.8}$$

In Eq. (8.7), $[E]^b$ is the bulk enzyme concentration and β is the dimensionless diffusion parameter (Schuck and Minton, 1996; Bourdillon et al., 1999) mentioned previously and defined by Eq. (8.9):

$$\beta = \frac{k_a\Gamma_{tot}}{k_m} = \frac{k_a\Gamma_{tot}\delta}{D} \tag{8.9}$$

These equations were derived in a series of recent papers (Fang et al., 2005; Lee et al., 2005b), and can be solved by simple Euler integration methods with the initial conditions $\theta_S = 1$ and $\theta_{ES} = \theta_{S*} = 0$ to yield three time-dependent surface coverages $\theta_{ES}(t)$, $\theta_{S*}(t)$, and $\theta_S(t)$. We have used these computer-generated solutions to Eqs. (8.6)–(8.8) to fit our SPRI measurements and obtain the four constants k_a, k_d, k_{cat}, and β (Fang et al., 2005; Lee et al., 2005b).

SPRI measurements are just one of few possible experimental methods that have been employed to monitor surface enzyme processes in real-time. While most research efforts have focused on the use of fluorescence based detection methods (Gaspers et al., 1994, 1995; Jervis et al., 1997; Tachi-iri et al., 2000; Bosma et al., 2003; Tawa and Knoll, 2004), SPR-based techniques are an alternative tool for measuring time-dependent surface coverages of the untagged adsorbing species that provides excellent discrimination against possible bulk signal contributions (Peterson et al., 2000, 2002; Goodrich et al., 2004b; Kanda et al., 2004; Shumaker-Parry and Campbell, 2004; Shumaker-Parry et al., 2004; Wegner et al., 2004b; Fang et al., 2005; Lee et al., 2005b).

Perhaps the most effective experimental method for the quantification of surface enzyme processes is to use a combination of SPR and fluorescence experiments. For example, Knoll and co-workers have recently used the combination of SPR and surface plasmon fluorescence spectroscopy (SPFS), which is a very sensitive fluorescence method for detecting labeled surface biochemical species (Yu et al., 2003; Tawa and Knoll, 2004; Yao et al., 2004; Stengel and Knoll, 2005). Kim et al. (2002) have also employed a combination of SPR and SPFS to create separate profiles of the enzyme adsorption and substrate cleavage steps. Moreover, we have recently demonstrated that the combination of time-resolved SPRI and SPFS measurements can be used for the study of RNase H hydrolysis of heteroduplexes on DNA microarrays (Fang et al., 2005).

Figure 8.9 plots the theoretical curves for $\theta_{ES}(t)$, $\theta_S(t)$, and $\theta_{S*}(t)$ for the reaction of a 2 nM RNase H solution with a monolayer of RNA–DNA heteroduplexes formed previously by the hybridization adsorption of ssRNA onto a ssDNA microarray element. These curves were obtained by fitting SPRI data to the solutions of Eqs. (8.6)–(8.8) (Fang et al., 2005).

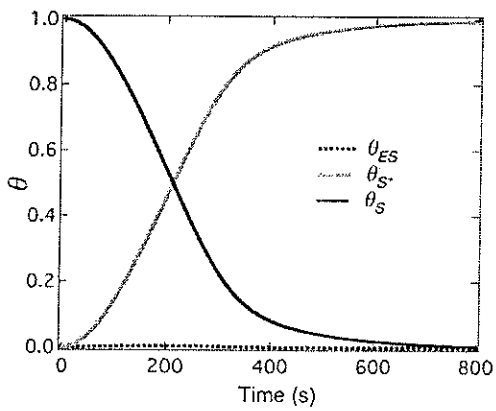

Figure 8.9. Theoretical analysis for the RNase H hydrolysis reaction of a surface immobilized RNA–DNA heteroduplex. The solid lines represent the simulated curves for $\theta_{ES}(t)$, $\theta_S(t)$, and $\theta_{S*}(t)$ obtained using Eqs. (8.6)–(8.8) with the parameters $k_a = 3.4 \times 10^6\ M^{-1}\ s^{-1}$, $[E]^b = 2$ nM, $k_d = 0.1\ s^{-1}$, $k_{cat} = 1.0\ s^{-1}$, and $\beta = 180$.

The values of the four reaction parameters in the model obtained from this fit are $k_a = 3.4 \times 10^6\ M^{-1}\ s^{-1}$, $k_d = 0.1\ s^{-1}$, $k_{cat} = 1.0\ s^{-1}$, and a diffusion parameter $\beta = 180$ for the SPRI measurements (Fang et al., 2005). Note that the enzyme–substrate complex coverage (θ_{ES}) remains very small throughout the course of the surface reaction. This is because the surface catalysis rate constant (k_{cat}) is much larger than the surface adsorption rate ($k_a[E]^b$), so that the enzyme reacts very quickly and is released from the surface. In fact, if we look at the Langmuir adsorption coefficient obtained from k_a and k_d ($K_{Ads} = 3.4 \times 10^7\ M^{-1}$), we find that $C_{0.5}$ is approximately 30 nM, so that even the equilibrium enzyme surface coverage would be low at a bulk target DNA concentration of 1 nM. However, the k_{cat} value of $1\ s^{-1}$ for RNase H is approximately 10 times slower than that observed for the RNase H reaction in solution (Hogrefe et al., 1990; Keck et al., 1998), so improvements in the surface attachment chemistry are still possible.

8.5. ULTRASENSITIVE DNA DETECTION WITH ENZYMATICALLY AMPLIFIED SPRI

General Methodology. Now that we have characterized the surface RNase H reaction, we are in the position to use this surface enzyme process to enhance the sensitivity of the SPRI measurements. A generalized surface destruction/amplification process that can be used on microarrays is depicted schematically in Figure 8.10. A surface containing attached probe molecules is exposed to a solution containing target molecules and an enzyme (e.g., RNase H, Exo III). After a target molecule binds to a probe molecule, the enzyme recognizes and binds to the surface-bound target–probe complex. The enzyme then destroys the probe, releasing both itself and the target molecule back into solution. The released target is now free to bind to another surface probe molecule, which can subsequently be destroyed by an enzyme molecule. The repeated target binding/enzymatic destruction/target release will result in a large amount of surface probe removal with a very small number of target molecules. This probe loss can be observed in the SPRI signal, although, in principle, this amplification methodology can work with a number of different surface-based detection techniques on various substrates.

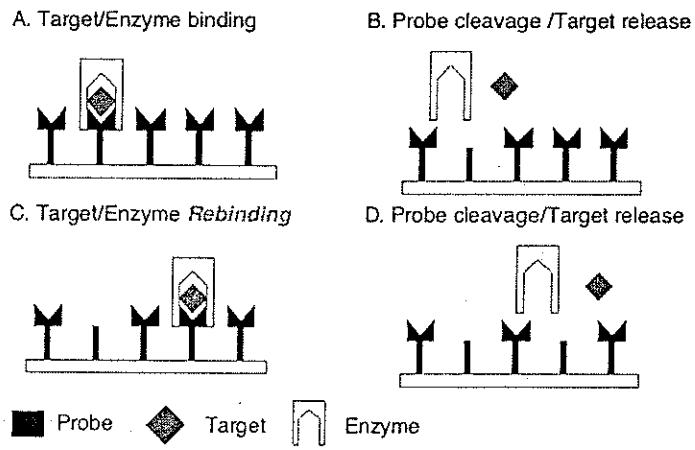

Figure 8.10. Schematic presentation of a general surface enzymatic amplification procedure.

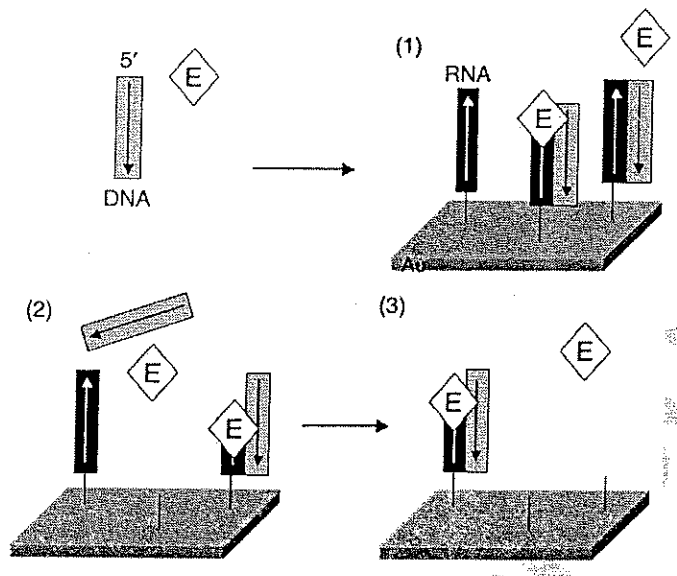

Figure 8.11. Schematic outlining the RNase H amplified SPRI detection of DNA using RNA microarrays.

This amplification method has been specifically applied to the RNase H hydrolysis of RNA microarrays (Goodrich et al., 2004a,b; Lee et al., 2005c), as well as to the Exo III hydrolysis of dsDNA microarrays (Lee et al., 2005a). Figure 8.11 shows the specific amplification scheme for the RNase H system. When the ssRNA microarray is exposed to a solution containing both target DNA and RNase H, the DNA will first bind to a complementary RNA molecule in a specific microarray element on the surface and form an RNA–DNA heteroduplex (step 1). RNase H will then bind to the heteroduplex and selectively hydrolyze the RNA probe. This hydrolysis process releases both the enzyme and the target DNA back into solution (step 2). The released DNA molecule is then free to bind to another RNA probe molecule in the same array element. Either the same RNase H molecule or a different one can bind to the new surface bound heteroduplex and again hydrolyze the probe RNA molecule (step 3). After a sufficient amount of time, a very small amount of target DNA can remove all of the RNA probe molecules from the surface with this cyclic binding and hydrolysis process.

Femtomolar Oligonucleotide Detection. To determine the sensitivity of enzymatically amplified SPRI measurements, we performed a number of experiments to detect ssDNA 16mers at various concentrations. Figure 8.12 shows an SPRI image (a) and line profile (c) obtained upon the hybridization adsorption of a target 16mer ssDNA (100 nM) onto ssRNA microarray elements in a two-component array (the second type of array element was a 16mer ssDNA negative control). A 1.7% increase in $\Delta\%R$ was observed upon hybridization adsorption as expected from the Langmuir adsorption isotherm. Also shown in Figure 8.12 are an SPRI image (b) and a line profile (c) taken after the microarray was exposed for 30 minutes to a solution containing 100 pM ssDNA and 16 nM of RNase H. A significant (–3.4%) loss in the SPRI signal was observed that almost equaled the loss observed from the solution of 500 nM ssDNA and RNase H as previously shown in Figure 8.7. Note that the sample signal loss obtained from the 100 pM DNA solution is substantially larger

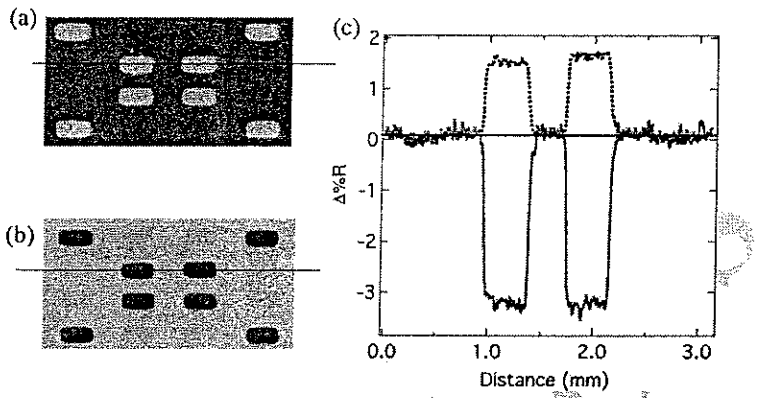

Figure 8.12. (a) An SPR difference image showing sequence specific hybridization of a 100 nM solution of target DNA onto ssRNA microarray elements. (b) An SPR image obtained by subtracting images taken before and after the ssRNA array was exposed to a solution containing 100 pM complementary target DNA and 8 nM RNase H for 30 minutes. (c) Comparison of line profiles in both images demonstrates the advantage of enzymatic amplification. The upper line profile shows an increase in percent reflectivity due to hybridization adsorption of target DNA, while a larger decrease in percent reflectivity is observed in the lower line profile using a much lower concentration (100 pM) of target DNA. The decrease in percent reflectivity corresponds to a complete removal of the ssRNA probes due to repeat cycles of hybridization adsorption of target DNA followed by enzyme hydrolysis.

than the meager $\Delta\%R$ gain observed from the 1 nM ssDNA solution without RNase H shown in Figure 8.5. Given enough time, both the 100 nM DNA solution and the 100 pM solution can completely remove all of the ssRNA from the surface in the presence of RNase H; however, the loss observed in the 500 nM DNA solution occurred at a substantially faster rate.

The initial rate of SPRI signal loss during the enzymatically amplified SPRI experiment can be used as a measure of the ssDNA target concentration. Figure 8.13 plots the time required to reach a 0.2% drop in percent reflectivity for an ssRNA microarray element as a

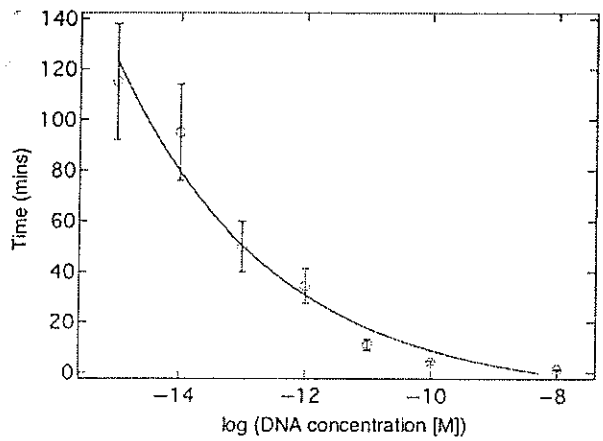

Figure 8.13. Plot of time required to reach an initial 0.2% change in reflectivity during RNase H hydrolysis versus a target DNA concentration ranging from 1 fM to 10 nM. [Reprinted with permission from *J Am Chem Soc* supporting materials 126:4086–4087. Copyright 2004, American Chemical Society.]

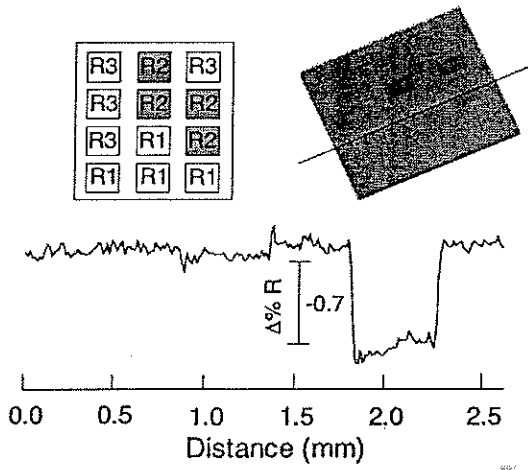

Figure 8.14. An SPR difference image showing the RNase H amplified detection of 1 fM 20mer target DNA using an RNA microarray. The top left is a schematic of the three-component RNA microarray. The line profile taken across the difference image shows a decrease in percent reflectivity ($-0.7\ \Delta\%R$) at the R2 probe elements only with no changes in the SPR signal observed at the R1 and R3 array elements. [Reprinted with permission from *J Am Chem Soc* **126**:4086–4087. Copyright 2004, American Chemical Society.]

function of target DNA concentration from 10 nM down to 1 fM in the presence of RNase H. As the concentration of target DNA decreases, the time required to reach this SPRI signal level becomes longer due to the drop in the surface concentration of heteroduplex. A linear relationship between target DNA concentration and time to reach a given loss in SPR signal was observed for concentrations from 1 fM to 10 pM. As expected, lower concentrations of DNA required more time to reach a desired SPR signal level due to the fact that more binding–hydrolysis cycles per DNA molecule were required. For a 10 pM ssDNA solution, 12 ± 2 minutes is required to observe a $-0.2\ \Delta\%R$; for 1 fM the time required was 120 ± 25 minutes. The lowest concentration detected with enzymatically amplified SPRI was an amazing 1 fM. To verify this detection limit, an SPRI reflectivity difference image was obtained from a three-component RNA microarray after approximately a 4-hour exposure to a solution containing a 1 fM 20mer target DNA complementary to only one of the three RNA array elements in the presence of RNase H (see Figure 8.14). A loss of $-0.7\ \Delta\%R$ was observed for this array element from this 1 fM solution of target DNA; no loss in SPRI was observed from the other two ssRNA microarray elements. This experiment attests to the very high selectivity and specificity of the surface RNase H reaction. Also note that the reaction time for the hydrolysis reaction is not determined by DNA diffusion to the surface, since the bulk solution is never depleted of target ssDNA. Instead, the time required for the signal loss is limited by the rate of ssDNA diffusion on the surface and the rates of hybridization adsorption and surface catalysis. The improvement of the detection limit from 1 nM for hybridization adsorption to 1 fM for enzymatically amplified SPR is a remarkable factor of 10^6! An estimate of the amount of enzymatic amplification achieved in this experiment was obtained from the stoichiometry of the experiment; 0.5 attomoles of complementary DNA were required to remove approximately 3 femtomoles of RNA probes, so on average every target molecule in solution removed approximately 6000 RNA probes from the surface.

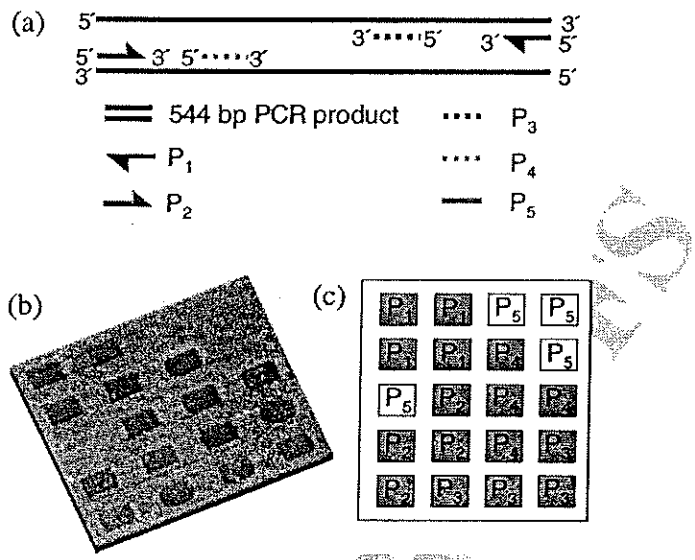

Figure 8.15. The RNase H amplified detection of a 544 bp PCR product of the TSPY gene. (a) Schematic showing the relative binding sites for probe molecule hybridization to the PCR product. (b) SPR difference image obtained by subtracting images taken before and 30 minutes after a 100 pM solution of the PCR product was exposed to the RNA array surface. A decrease in percent reflectivity was observed for the array elements (P_1, P_2, P_3, and P_4) designed to bind to the PCR product. P_5 serves as a negative control. (c) Schematic showing the five-component RNA microarray. [Reprinted with permission from *Anal Chem* 76:6173–6178. Copyright 2004, American Chemical Society.]

PCR Product Detection. In addition to single-stranded oligonucleotides, enzymatically amplified SPRI can also be used to detect longer strands of dsDNA such as those created by the PCR amplification of a genomic DNA sample. A 544-bp segment of the TSPY gene was obtained from human genomic DNA by PCR amplification (Goodrich et al., 2004b). A five-component RNA array was constructed with probe sequences P_1–P_4 designed to specifically bind to the TSPY PCR product, and P_5 was used as a negative control (see Figure 8.15c). The location of the binding sites for the four probes on the PCR product is shown in Figure 8.15a. A sized and purified sample of the PCR product was then diluted to a concentration of 100 pM and heated to 95°C for 5 minutes to denature the duplexed DNA strands. RNase H was then added to the DNA solution, which was then injected into the 100 μL cell in contact with the RNA microarray surface. Figure 8.15b shows the SPRI differential reflectance image obtained from this experiment; a decrease in percent reflectivity can be seen for all of the probes that were designed to specifically bind to this PCR product, while the P_5 negative control array element showed no change. This experiment illustrates that the RNase H surface enzymatic process can be used to detect longer dsDNA PCR products; the SPRI image obtained from a 100 pM solution of unpurified products gave similar results (Goodrich et al., 2004b).

Direct Detection of Genomic DNA. Finally, the sensitivity of enzymatically amplified SPRI is actually sufficient to directly detect genomic DNA *without* PCR amplification. A three-component RNA microarray was constructed with two RNA probe sequences designed to bind to the TSPY gene (R1 and R2 in Figure 8.16), and a third negative control RNA sequence (R3). Male and female genomic DNA samples were obtained commercially,

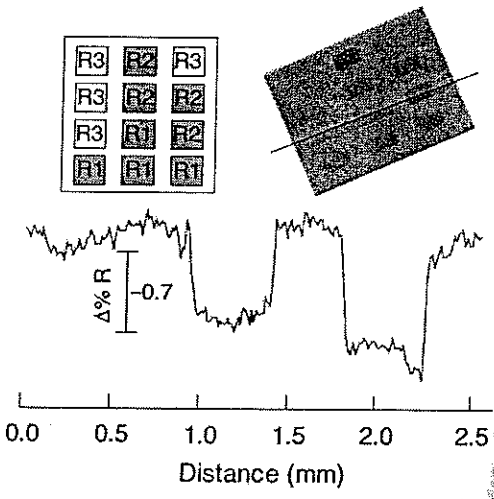

Figure 8.16. An SPR difference image obtained for the detection of 7 fM male genomic DNA using the RNase H amplification method. The upper left inset shows the pattern of the three-component array with the RNA probes R1 and R2 designed to selectively bind to the TSPY gene on the Y chromosome with R3 used as a negative control. The line profile displays a decrease in percent reflectivity for the R1 and R2 array elements where hybridization adsorption followed by RNA probe hydrolysis occurred. [Reprinted with permission from *J Am Chem Soc* **126**:4086–4087. Copyright 2004, American Chemical Society.]

sheared by vortexing and sonication, diluted in buffer, heated to 95°C for 5 min, and then mixed with RNase H. The concentration of the TSPY gene sequences in the male genomic DNA used was estimated to be 7 fM (Goodrich et al., 2004a). The array was then exposed to the genomic DNA for approximately 4 hours and the SPR reflectance difference image in Figure 8.16 was obtained. A significant decrease in SPRI signal (–0.7%) was observed for the two probes specific for the TSPY gene, while no SPRI signal loss was observed in either the negative control or background. As a control, enzymatically amplified SPRI experiments were performed on female genomic DNA under the same conditions; no decrease in SPRI signal from any of the array elements was observed. These experiments unequivocally demonstrate that enzymatically amplified SPRI can be used to directly detect specific DNA sequences from genomic samples.

8.6. SUMMARY AND OUTLOOK

The ability to sensitively detect and identify multiple DNA or RNA sequences in a microarray format without the use of labeling can greatly assist in many ongoing biosensing applications including gene expression analysis, biowarfare detection, and viral identification. The enzymatically amplified SPRI detection described in this chapter highlights the potential of enzymes as invaluable surface bioengineering tools for use in the development of novel microarray-based biosensing methodologies. Other examples of surface enzyme reactions implemented with multielement surface biosensors include ligation (Gerry et al., 1999; Broude et al., 2001; Zhong et al., 2003; Deng et al., 2004), primer extension (Hultin et al., 2005), and single base extension reactions (Giusto and King, 2003) for single nucleotide polymorphism detection.

The most widely used method for the detection and identification of DNA or RNA using DNA microarrays is fluorescence imaging, which has a detection limit typically in the region of 1–10 pM (Zammatteo et al., 2000; Lehr et al., 2003; Livache et al., 2003). Therefore, in order to use this method for the detection of femtomolar DNA concentrations—for example, in genomic DNA studies—enzymatic amplification methods such as PCR are commonly used prior to array exposure (Sengupta et al., 2003; Gonzalez et al., 2004). Alternatively, coupled enzymatic labeling methods such as an ELISA sandwich assay can be used after target adsorption (Kawai et al., 1993; Morata et al., 2003). However, these enzymatic amplification methods are not readily adapted to a multiplexed array format; PCR requires multiple primers for multiple target DNA and is often unable to reproduce the relative concentrations of nucleic acid sequences from complex mixtures, while the enzymatic product detected in ELISA measurements is a solution species that can diffuse into neighboring array elements. An alternative strategy for the ultrasensitive detection of DNA using DNA microarrays is the use of nanoparticle tagging in a sandwich assay format (Storhoff et al., 2004; Bao et al., 2005). In these cases, a 50–200 fM detection limit was achieved only after a second silver staining amplification step.

In this chapter, we have demonstrated that the sensitivity of SPRI for the direct detection and identification of DNA can be lowered down to 1 fM by monitoring the repeated enzymatic hydrolysis of surface RNA–DNA heteroduplexes by RNase H. This method of "enzymatically amplified SPRI" is an extraordinary improvement compared to the nanomolar DNA detection limit of SPRI based solely on hybridization adsorption. This method is successful because one target DNA molecule can destroy multiple surface bound RNA molecules. The technique can be used to directly detect oligonucleotides, PCR fragments, and sequences in unamplified genomic DNA, and will work with all DNA sequences that can form DNA–RNA heteroduplexes (Goodrich et al., 2004a,b). Furthermore, this enzymatic amplification method can be used in conjunction with other detection methods such as fluorescence and electrochemical measurements for even more sensitive DNA detection, perhaps with the ability to detect single molecular binding events.

Although the RNase H amplification technique offers excellent sensitivity and selectivity, it requires the use of an RNA microarray. At present, there are only a few reports on the creation of RNA microarrays currently available in the literature (McCauley et al., 2003; Goodrich et al., 2004a,b; Collett et al., 2005; Lee et al., 2005c). Special care is required during RNA microarray fabrication in order to avoid degradation of the RNA either by nucleases from environmental sources or during the chemical processing of the surface. The design of new array fabrication strategies that require very little *ex situ* handling or chemical processing of the RNA remains a significant challenge that, if met, will greatly promote the application of RNA microarrays in a number of research areas.

Finally, the surface enzyme reaction can be orders of magnitude slower on a surface as compared to that in solution. The surface density, orientation, and spacing from the chip surface of the immobilized substrate as well as the enzyme–substrate binding affinity are some of the many energetic and transport factors that can greatly affect enzymatic activity on a surface. The application of powerful *in situ* surface analytical surface techniques that can directly monitor enzyme activity in combination with a good theoretical understanding is essential for the optimization of these new surface enzymatic based techniques. To date, there are very few quantitative studies considering the kinetics and thermodynamics of enzyme-catalyzed reactions on surfaces; further investigation into these fundamental research areas will undoubtedly accelerate the harnessing of the unique properties of enzymes for ultrasensitive biosensing applications.

ACKNOWLEDGMENT

This research is funded by the National Institute of Health (2RO1 GM059622-04) and the National Science Foundation (CHE-0133151).

REFERENCES

Bao, YP, Martin Huber, M, Wei, T, Marla, SS, Storhoff, JJ, and Müller, UR (2005). SNP identification in unamplified human genomic DNA with gold nanoparticle probes. *Nucleic Acids Res* **33**:e15.

Berchuck, A, Iversen, ES, Lancaster, JM, Pittman, J, Luo, J, Lee, P, Murphy, S, Dressman, HK, Febbo, PG, West, M, Nevins, JR, and Marks, JR (2005). Patterns of gene expression that characterize long-term survival in advanced stage serous ovarian cancers. *Clin Cancer Res* **11**:3686–3696.

Bosma, AY, Ulijn, RV, McConnell, G, Girkin, J, Hallinge, PJ, and Flitsch, SL (2003). Using two photon microscopy to quantify enzymatic reaction rates on polymer beads. *Chem Commun* **22**:2790–2791.

Bourdillon, C, Demaille, C, Moiroux, J, and Saveant, J (1999). Activation and diffusion in the kinetics of adsorption and molecular recognition on surfaces. Enzyme-amplified electrochemical approach to biorecognition dynamics illustrated by the binding of antibodies to immobilized antigens. *J Am Chem Soc* **121**:2401–2408.

Brenner, S, Johnson, M, Bridgham, J, Golda, G, Lloyd, DH, Johnson, D, Luo, S, McCurdy, S, Foy, M, Ewan, M, Roth, R, George, D, Eletr, S, Albrecht, G, Vermaas, E, Williams, SR, Moon, K, Burcham, T, Pallas, M, DuBridge, RB, Kirchner, J, Fearon, K, Mao, J, and Corcoran, K (2000). Gene expression analysis by massively parallel signature sequencing (MPSS) on microbead arrays. *Nat Biotechnol* **18**:630–634.

Brockman, JM, Frutos, AG, and Corn, RM (1999). A multistep chemical modification procedure to create DNA arrays on gold surfaces for the study of protein–DNA interactions with surface plasmon resonance imaging. *J Am Chem Soc* **121**:8044–8051.

Brockman, JM, Nelson, BP, and Corn, RM (2000). Surface plasmon resonance imaging measurements of ultrathin organic films. *Annu Rev Phys Chem* **51**:41–63.

Broude, NE, Woodward, K, Cavallo, R, Cantor, CR, and Englert, D (2001). DNA microarrays with stem–loop DNA probes: Preparation and applications. *Nucleic Acids Res* **29**:e92.

Chen, CC, Teng, LJ, Kaiung, S, and Chang, TC (2005). Identification of clinically relevant viridans streptococci by an oligonucleotide array. *J Clin Microbiol* **43**:1515–1521.

Chinowsky, TM, Quinn, JG, Bartholomew, DU, Kaiser, R, and Elkind, JL (2003). Performance of the Spreeta 2000 integrated surface plasmon resonance affintiy sensor. *Sens Actuators B* **91**:266–274.

Collett, JR, Cho, EJ, Lee, JF, Levy, M, Hood, AJ, Wan, C, and Ellington, AD (2005). Functional RNA microarrays for high-throughput screening of antiprotein aptamers. *Anal Biochem* **338**:113–123.

Corn, RM, and Weibel, SC (2001). Fourier transform surface plasmon resonance. In: Chalmers, J, and Griffiths, PR (eds.), *Handbook of Vibrational Spectroscopy*, Vol. 2. John Wiley & Sons, New York, pp. 1057–1064.

Crowther, JR (1995). ELISA: Theory and practice. In: Crowther, JR (ed.), *Methods in Molecular Biology*, Vol. 42. Humana Press, Totowa, NJ.

Deng, J, Zhang, X, Manga, Y, Zhang, Z, Zhou, Y, Liu, Q, Lu, H, and Fu, Z (2004). Oligonucleotide ligation assay-based DNA chip for multiplex detection of single nucleotide polymorphism. *Biosens Bioelectron* **19**:1277–1283.

Epstein, JR, Biran, I, and Walt, DR (2002). Fluorescence-based nucleic acid detection and microarrays. *Anal Chim Acta* **469**:3–36.

Au: Update?
Fang, S, Lee, HJ, Wark, AW, Kim, HM, and Corn, RM (2005). Determination of ribonuclease H surface enzyme kinetics by surface plasmon resonance imaging and surface plasmon fluorescence spectroscopy. *Anal Chem* **00**:000–000.

Frutos, AG, Weibel, SC, and Corn, RM (1999). Near infrared surface plasmon resonance measurements of ultrathin films. 2. Fourier transform SPR spectroscopy. *Anal Chem* **71**:3935–3940.

Gaspers, PB, Robertson, CR, and Gast, AP (1994). Enzymes on immobilized substrate surfaces: Diffusion. *Langmuir* **10**:2699–2704.

Gaspers, PB, Gast, AP, and Robertson, CR (1995). Enzymes on immobilized substrate surfaces: reaction. *J Colloid Interface Sci* **172**:518–529.

Gerion, D, Chen, F, Kannan, B, Fu, A, Parak, WJ, Chen, DJ, Majumdar, A, and Alivisatos, AP (2003). Room-temperature single-nucleotide polymorphism and multiallele DNA detection using fluorescent nanocrystals and microarrays. *Anal Chem* **75**:4766–4772.

Gerry, NP, Witowski, NE, Day, J, Hammer, RP, Barany, G, and Barany, F (1999). Universal DNA microarray method for multiplex detection of low abundance point mutations. *J Mol Biol* **292**:251–262.

Giusto, DD, and King, GC (2003). Single base extension (SBE) with proofreading polymerases and phosphorothioate primers: Improved fidelity in single-substrate assays. *Nucleic Acids Res* **31**:e7.

Gonzalez, SF, Krug, MJ, Nielsen, ME, Santos, Y, and Call, DR (2004). Simultaneous detection of marine fish pathogens by using multiplex PCR and DNA microarrays. *J Clin Microbiol* **42**:1414–1419.

Goodrich, TT, Lee, HJ, and Corn, RM (2004a). Direct detection of genomic DNA by enzymatically amplified SPR imaging measurements of RNA microarrays. *J Am Chem Soc* **126**:4086–4087.

Goodrich, TT, Lee, HJ, and Corn, RM (2004b). Enzymatically amplified surface plasmon resonance imaging method using RNase H and RNA microarrays for the ultrasensitive detection of nucleic acids. *Anal Chem* **76**:6173–6178.

Guedon, P, Livache, T, Martin, F, Lesbre, F, Roget, A, Bidan, G, and Levy, Y (2000). Characterization and optimization of a real-time, parallel, label-free, polypyrrole-based DNA sensor by surface plasmon resonance imaging. *Anal Chem* **72**:6003–6009.

Hanken, DG, Jordan, CE, Frey, BL, and Corn, RM (1998). Surface plasmon resonance measurements of ultrathin organic films at electrode surfaces. In: Bard, A, and Rubinstein, I (eds.), *Electroanalytical Chemistry: A Series of Advances*, Vol. 20, Marcel Dekker, New York, pp. 141–225.

He, L, Musick, MD, Nicewarner, SR, Salinas, FG, Benkovic, SJ, Natan, MJ, and Keating, CD (2000). Colloidal Au-enhanced surface plasmon resonance for ultrasensitive detection of DNA hybridization. *J Am Chem Soc* **122**:9071–9077.

Hogrefe, HH, Hogrefe, RI, Walder, RY, and Walder, JA (1990). Kinetic analysis of *Escherichia coli* RNase H using DNA–RNA–DNA/DNA substrates. *J Biol Chem* **265**:5561–5566.

Homola, J, Yee, SS, and Gauglitz, G (1999). Surface plasmon resonance sensors: Review. *Sens Actuators B* **54**:3–15.

Hughes, TR, Mao, M, Jones, A, Burchard, J, Marton, MJ, Shannon, KW, Lefkowitz, SM, Ziman, M, Schelter, JM, Meyer, MR, Kobayashi, S, Davis, C, Dai, H, He, YD, Stephaniants, SB, Cavet, G, Walker, WL, West, A, Coffey, E, Shoemaker, DD, Stoughton, R, Blanchard, AP, Friend, SH, and Linsley, PS (2001). Expression profiling using microarrays fabricated by an ink-jet oligonucleotide synthesizer. *Nat Biotechnol* **19**:342–347.

Au: Cite in text.
Hultin, E, Kaller, M, Ahmadian, A, and Lundeberg, J (2005). Competitive enzymatic reaction to control allele-specific extensions. *Nucleic Acids Res* **33**:e48.

Jervis, EJ, Haynes, CA, and Kilburn, DG (1997). Surface diffusion of cellulases and their isolated binding domains on cellulose. *J Biol Chem* **272**:24016–24023.

Kanda, V, Kariuki, JK, Harrison, DJ, and McDermott, MT (2004). Label-free reading of microarray-based immunoassays with surface plasmon resonance imaging. *Anal Chem* **76**:7257–7262.

Katayanagi, K, Okumura, M, and Morikawa, K (1993). Crystal structure of escherichia coli RNase HI in complex with Mg^{2+} at 2.8 Å resolution: Proof for a single Mg^{2+} binding site. *Proteins: Struct Funct Genet* **17**:337–346.

Kawai, S, Maekawajiri, S, and Yamane, A (1993). A simple method of detecting amplified DNA with immobilized probes on microtiter wells. *Anal Biochem* **209**:63–69.

Keck, JL, Goedken, ER, and Marqusee, S (1998). Activation/attenuation model for RNase H. *J Biol Chem* **273**:34128–34133.

Kim, J-H, Roy, S, Kellis, JT, Jr., Poulose, AJ, Gast, AP, and Robertson, CR (2002). Protease adsorption and reaction on an immobilized substrate surface. *Langmuir* **18**:6312–6318.

Knoll, W (1998). Interfaces and thin films as seen by bound electromagnetic waves. *Annu Res Phys Chem* **49**:569–638.

Kwok, P-Y (2001). Methods for genotyping single nucleotide polymorphisms. *Annu Rev Genomics Hum Genet* **2**:235–258.

Kyo, M, Yamamoto, T, Motohashi, H, Kamiya, T, Kuroita, T, Tanaka, T, Engel, JD, Kawakami, B, and Yamamoto, M (2004). Evaluation of MafG interaction with Maf recognition element arrays by surface plasmon resonance imaging technique. *Genes to Cells* **9**:153–164.

Lee, HJ, Goodrich, TT, and Corn, RM (2001). SPR imaging measurements of 1-D and 2-D DNA microarrays created from microfluidic channels on gold thin films. *Anal Chem* **73**:5525–5531.

Lee, HJ, Li, Y, Wark, AW, and Corn, RM (2005a). Enzymatically amplified SPR imaging detection of DNA by exonuclease III digestion of DNA microarrays. *Anal Chem* **77**:5096–5100.

Lee, HJ, Wark, AW, Goodrich, TT, Fang, S, and Corn, RM (2005b). Surface enzyme kinetics for biopolymer microarrays: A combination of Langmuir and Michaelis–Menten concepts. *Langmuir* **21**:4050–4057.

Lee, HJ, Wark, AW, Li, Y, and Corn, RM (2005c). Fabrication of renewable RNA microarrays by RNA–DNA surface ligation for enzymatically amplified SPR imaging. *J Am Chem Soc*, submitted for publication.

Au: Update.

Lee, HJ, Yan, Y, Marriott, G, and Corn, RM (2005d). Quantitative functional analysis of protein complexes on surfaces. *J Physiol* **563**:61–71.

Lehr, H-P, Reimann, M, Brandenburg, A, Sulz, G, and Klapproth, H (2003). Real-time detection of nucleic acid interactions by total internal reflection fluorescence. *Anal Chem* **75**:2414–2420.

Levicky, R, and Horgan, A (2005). Physicochemical perspectives on DNA microarray and biosensor technologies. *Trends Biotechnol* **23**:143–149.

Liebermann, T, Knoll, W, Sluka, P, and Herrmann, R (2000). Complement hybridization from solution to surface-attached probe-oligonucleotides observed by surface-plasmon-field-enhanced fluorescence spectroscopy. *Colloids Surf A* **169**:337–350.

Lin, B, Vora, GJ, Thach, D, Walter, E, Metzgar, D, Tibbetts, C, and Stenger, DA (2004). Use of oligonucleotide microarrays for rapid detection and serotyping of acute respiratory disease-associated adenoviruses. *J Clin Microbiol* **42**:3232–3239.

Livache, T, Maillart, E, Lassalle, N, Mailley, P, Corso, B, Guedon, P, Roget, A, and Levy, Y (2003). Polypyrrole based DNA hybridization assays: Study of label free detection processes versus fluorescence on microchips. *J Pharm Biomed Anal* **32**:687–696.

Lockhart, DJ, and Winzeler, EA (2000). Genomics, gene expression and DNA arrays. *Nature* **405**:827–836.

Lyon, LA, Holliway, WD, and Natan, MJ (1999). An improved surface plasmon resonance imaging apparatus. *Rev Sci Instrum* **70**:2076–2081.

McCauley, TG, Hamaguchi, N, and Stanton, M (2003). Aptamer-based biosensor arrays for detection and quantification of biological macromolecules. *Anal Biochem* **319**:244–250.

Morata, P, Queipo-Ortuno, MI, Reguera, JM, Garcia-Ordonez, MA, Cardenas, A, and Colmenero, JD (2003). Development and evaluation of a PCR-enzyme-linked immunosorbent assay for diagnosis of human brucellosis. *J Clin Microbiol* **41**:144–148.

Nakamura, H, Oda, Y, Iwai, S, Inoue, H, Ohtsuka, E, Kanaya, S, Kimura, S, Katsuda, C, Katayangi, K, Morikawa, K, Miyashiro, H, and Ikehara, M (1991). How does RNase H recognize a DNA–RNA hybrid. *Proc Natl Acad Sci USA* **88**:11535–11539.

Nelson, BP, Grimsrud, TE, Liles, MR, Goodman, RM, and Corn, RM (2001). Surface plasmon resonance imaging measrements of DNA and RNA hybridization adsorption onto DNA microarrays. *Anal Chem* **73**:1–7.

Nelson, BP, Liles, MR, Frederick, K, Goodman, RM, and Corn, RM (2002). Label-free detection of 16s rRNA hybridization onto DNA arrays using surface plasmon resonance imaging. *Environ Microbiol* **4**:735–743.

Nelson, PT, Baldwin, DA, Scearce, LM, Oberholtzer, JC, Tobias, JW, and Mourelatos, Z (2004). Microarray-based, high-throughput gene expression profiling of microRNAs. *Nature Methods* **1**:155–161.

Okumura, A, Sato, Y, Kyo, M, and Kawaguchi, H (2005). Point mutation detection with the sandwich method employing hydrogel nanospheres by the surface plasmon resonance imaging technique. *Anal Biochem* **339**:328–337.

Pease, AC, Solas, D, Sullivan, EJ, Cronin, MT, Holmes, CP, and Fodor, SPA (1994). Light-generated oligonucleotide arrays for rapid DNA sequence analysis. *Proc Natl Acad Sci USA* **91**:5022–5026.

Peterson, AW, Heaton, RJ, and Georgiadis, RM (2000). Kinetic control of hybridization in surface immobilized DNA monolayer films. *J Am Chem Soc* **122**:7837–7838.

Peterson, AW, Wolf, LK, and Georgiadis, RM (2002). Hybridization of mismatched or partially matched DNA at surfaces. *J Am Chem Soc* **124**:14601–14607.

Rella, R, Spadavecchia, J, Manera, MG, Siciliano, P, Santino, A, and Mita, G (2004). Liquid phase SPR imaging experiments for biosensors applications. *Biosens Bioelectron* **20**:1140–1148.

Schena, M, Shalon, D, Davis, RW, and Brown, PO (1995). Quantitative monitoring of gene expression patterns with a complementary DNA microarray. *Science* **270**:467–470.

Schuck, P, and Minton, AP (1996). Analysis of mass transport-limited binding kinetics in evanescent wave biosensors. *Anal Biochem* **240**:262–272.

Sengupta, S, Onodera, K, Lai, A, and Melcher, U (2003). Molecular detection and identification of influenza viruses by oligonucleotide microarray hybridization. *J Clin Microbiol* **41**:4542–4550.

Shumaker-Parry, JS, and Campbell, CT (2004). Quantitative methods for spatially resolved adsorption/desorption measurements in real time by surface plasmon resonance microscopy. *Anal Chem* **76**:907–917.

Shumaker-Parry, JS, Zareie, MH, Aebersold, R, and Campbell, CT (2004). Microspotting streptavidin and double stranded DNA arrays on gold for high-throughput studies of protein–DNA interactions by surface plasmon resonance microscopy. *Anal Chem* **76**:918–929.

Smith, EA, Kyo, M, Kumasawa, H, Nakatani, K, Saito, I, and Corn, RM (2002). Chemically induced hairpin formation in DNA monolayers. *J Am Chem Soc* **124**:6810–6811.

Smith, EA, and Corn, MR (2003). Surface plasmon resonance imaging as a tool to monitor biomolecular interactions in an array based format. *Appl Spectrosc* **57**:320A–332A.

Smith, EA, Erickson, MG, Ulijasz, AT, Weisblum, B, and Corn, RM (2003a). Surface plasmon resonance imaging of transcription factor proteins: Interactions of bacterial response regulators with DNA arrays on gold films. *Langmuir* **19**:1486–1492.

Smith, EA, Thomas, WD, Kiessling, LL, and Corn, RM (2003b). Surface plasmon resonance imaging studies of protein–carbohydrate interactions. *J Am Chem Soc* **125**:6140–6148.

Stears, RL, Martinsky, T, and Schena, M (2003). Trends in microarray analysis. *Nat Med* **9**:140–145.

Stengel, G, and Knoll, W (2005). Surface plasmon field-enhanced fluorescence spectroscopy studies of primer extension reactions. *Nucleic Acids Res* **33**:e69.

Storhoff, JJ, Marla, SS, Bao, P, Hagenow, S, Mehta, H, Lucas, A, Garimella, V, Patno, T, Buckingham, W, Cork, W, and Müller, UR (2004). Gold nanoparticle-based detection of genomic DNA targets on microarrays using a novel optical detection system. *Biosens Bioelectron* **19**:875–883.

Stoughton, RB (2005). Applications of DNA microarrays in biology. *Annu Rev Biochem* **74**:53–82.

Szabo, A, Stolz, L, and Granzow, R (1995). Surface plasmon resonance and its use in biomolecular interaction analysis (BIA). *Curr Opin Struct Biol* **5**:699–705.

Tachi-iri, Y, Ishikawa, M, and Hirano, K.-i. (2000). Investigation of the hydrolysis of single DNA molecules using fluorescence video microscopy. *Anal Chem* **72**:1649–1656.

Tawa, K, and Knoll, W (2004). Mismatching base-pair dependence of the kinetics of DNA–DNA hybridization studied by surface plasmon fluorescence spectroscopy. *Nucleic Acids Res* **32**:2372–2377.

Thomson, JM, Parker, J, Perou, CM, and Hammond, SM (2004). A custom microarray platform for analysis of microRNA gene expression. *Nature Methods* **1**:47–53.

van Hal, NLW, Vorst, O, van Houwelingen, AMML, Kok, EJ, Peijnenburg, A, Aharoni, A, van Tunen, AJ, and Keijer, J (2000). The application of DNA microarrays in gene expression analysis. *J Biotechnol.* **78**:271–280.

Volokhov, D, Chizhikov, V, Chumakov, K, and Rasooly, A (2003). Microarray-based identificaiton of thermophilic *Campylovacter jejuni*, *C. coli*, *C. lari*, and *C. upsaliensis*. *J Clin Microbiol* **41**:4071–4080.

Wang, D, Coscoy, L, Zylberberg, M, Avila, PC, Boushey, HA, Ganem, D, and DeRisi, JL (2002). Microarray-based detection and genotyping of viral pathogens. *Proc Natl Acad Sci USA* **99**:15687–15692.

Wark, AW, Lee, HJ, and Corn, RM (2005). Long-range surface plasmon resonance imaging for bioaffinity sensors. *Anal Chem* **77**:3904–3907.

Wegner, GJ, Lee, HJ, and Corn, RM (2002). Characterization and optimization of peptide arrays for the study of epitope–antibody interactions using surface plasmon resonance imaging. *Anal Chem* **74**:5161–5168.

Wegner, GJ, Lee, HJ, Marriott, G, and Corn, RM (2003). Fabrication of histidine-tagged fusion protein arrays for surface plasmon resonance imaging studies of protein–protein and protein–DNA interactions. *Anal Chem* **75**:4740–4746.

Wegner, GJ, Lee, HJ, and Corn, RM (2004a). Surface plasmon resonance imaging measurements of DNA, RNA, and protein interactions to biomolecular arrays. In: Kambhampati, D. (ed.), *Protein Microarray Technology*. Wiley-VCH, Weinheim, pp. 107–129.

Wegner, GJ, Wark, AW, Lee, HJ, Codner, E, Saeki, T, Fang, S, and Corn, RM (2004b). Real-time SPR imaging measurements for the multiplexed determination of protein adsorption/desorption kinetics and surface enzymatic reactions on peptide microarrays. *Anal Chem* **76**:5677–5684.

Wilkop, T, Wang, Z, and Cheng, Q (2004). Analysis of μ-contact printed protein patterns by SPR imaging with a LED light source. *Langmuir* **20**:11141–11148.

Winzeler, EA, Richards, DR, Conway, AR, Goldstein, AL, Kalman, S, McCullough, MJ, McCusker, JH, Stevens, DA, Wodicka, L, Lockhart, DJ, and Davis, RW (1998). Direct allelic variation scanning of the yeast genome. *Science* **281**:1194–1197.

Yao, D, Yu, F, Kim, J, Scholz, J, Nielsen, PE, Sinner, E, and Knoll, W (2004). Surface plasmon field-enhanced fluorescence spectroscopy in PCR product analysis by peptide nucleic acid probes. *Nucleic Acids Res* **32**:e177.

Yu, F, Yao, D, and Knoll, W (2003). Surface plasmon field-enhanced fluorescence spectroscopy studies of the interaction between an antibody and its surface-coupled antigen. *Anal Chem* **75**:2610–2617.

Zamaratski, E, Pradeepkumar, PI, and Chattopadhyaya, J (2001). A critical survey of the structure–function of the antisense oligo/RNA heteroduplex as substrate for RNase H. *J Biochem Biophys Methods* **48**:189–208.

Zammatteo, N, Jeanmart, L, Hamels, S, Courtois, S, Louette, P, Hevesi, L, and Remacle, J (2000). Comparison between different strategies of covalent attachment of DNA to glass surfaces to build DNA microarrays. *Anal Biochem* **280**:143–150.

Zhong, X, Reynolds, R, Kidd, JR, Kidd, KK, Jenison, R, Marlar, RA, and Ward, DC (2003). Single-nucleotide polymorphism genotyping on optical thin-film biosensor chips. *Proc Natl Acad Sci USA* **100**:11559–11564.